The dissociative adsorption of N_2 on a multiply promoted iron catalyst used for ammonia synthesis: a temperature-programmed desorption study

M. Muhler [1], F. Rosowski and G. Ertl

Fritz-Haber-Institut der Max-Planck-Gesellschaft, Faradayweg 4-6, D-14195 Berlin (Dahlem), Germany

Received 4 August 1993; accepted 4 November 1993

The temperature-programmed desorption (TPD) of N_2 from a multiply promoted iron catalyst used for ammonia synthesis has been studied in a microreactor system at atmospheric pressure. From TPD experiments with various heating rates a preexponential factor $A = 2 \times 10^9$ molecules/site s and an activation energy $E = 146$ kJ/mol was derived assuming second-order desorption. The observed dependence of the TPD peak shapes on the heating rates indicated the influence of readsorption of N_2 in agreement with the results obtained for various initial coverages. Simulating the N_2 TPD curves using the model by Stoltze and Nørskov revealed that the calculated TPD curves were not influenced by the molecular precursor to desorption. However, the calculated rate of readsorption was found to be overestimated at high coverage compared with the experimental results. A coverage-dependent net activation energy for dissociative chemisorption (E^*) was introduced as the simplest assumption rendering the dissociative chemisorption of N_2 activated at high coverage. The best fit of the experimental data yielded $E^* = (-15 + 30\theta)$ kJ/mol using only a single type of atomic nitrogen species. These findings are in satisfactory agreement with the parameters underlying the Stoltze–Nørskov model for the kinetics of ammonia synthesis as well as with the data reported for Fe(111) single crystal surfaces.

Keywords: Nitrogen adsorption; N_2 TPD; iron-based catalyst; ammonia synthesis; microkinetic analysis

1. Introduction

In spite of intensive research on the mechanism of ammonia synthesis over iron catalysts [1], there is an ongoing debate on the detailed kinetics of the dissociative adsorption of N_2 which is generally accepted to be the rate-determining step [2]. The active catalyst surface is assumed to consist predominantly of Fe(111) planes

[1] To whom correspondence should be addressed.

[2,3]. By varying the surface temperature only, the dissociative adsorption of N_2 on clean Fe(111) studied under ultra-high vacuum (UHV) conditions with N_2 dosing pressures up to 10^{-4} mbar was concluded to be non-activated [4–7]. On the other hand, it was suggested that a net activation barrier of 50 kJ/mol exists on iron catalysts under industrial synthesis conditions due to the high coverage of adsorbed atomic nitrogen (N_{ads}) [8–11]. The molecular beam studies by Rettner and Stein [12,13] revealed a strong energy dependence of the initial sticking probability of N_2 on Fe(111) indicating that in addition to the crystal surface temperature dependence measured by Ertl et al. [4–7] also a considerable gas temperature dependence has to be taken into account.

Recently, in this laboratory a N_2 temperature-programmed desorption (TPD) study carried out at low temperature in UHV demonstrated that the desorption traces of molecular nitrogen observed for an industrial ammonia catalyst were quite similar to those recorded with a K promoted Fe(111) surface [3]. Vandervell and Waugh [14] reinvestigated the role of potassium and alumina by studying H_2 and N_2 TPD from promoted iron catalysts in a microreactor system and arrived at contradicting conclusions. However, the application of TPD in a flow system is not without pitfalls as demonstrated in ref. [15]. In their latest study Waugh et al. [16] were able to observe all three expected N_2 desorption states at low temperature from a triply promoted catalyst.

Contrary to TPD studies with flat single crystal surfaces in UHV additional effects due to readsorption of the desorbed molecules within the catalyst bed may occur rendering the interpretation of the TPD traces less straightforward. In this case the resulting shape of the TPD trace is determined both by the desorption kinetics and the adsorption kinetics. It is the purpose of the present N_2 TPD study to demonstrate how the kinetic parameters for adsorption and desorption can be extracted from series of TPD experiments with varying heating rates and initial coverages by means of a microkinetic analysis. These kinds of experiments are considered to be crucial tests for the applicability of kinetic data derived from single crystal studies in UHV to microkinetic modelling under industrial conditions. The shape of the N_2 TPD spectrum should, in addition, also reflect the participation of different crystallographic planes since N_{ads} is known to have different activation energies for desorption on Fe(111), Fe(100) and Fe(110) [4,5]. In the case of copper-based catalysts recent H_2 TPD experiments offered the possibility to evaluate the morphology of the Cu particles [17].

The present microkinetic analysis is based on the kinetic simulation of ammonia synthesis by Stoltze and Nørskov [18–20] using the approach by Dumesic and Trevino [21]. Adsorption and desorption of N_2 involve schematically the following steps:

$$N_2 + * \underset{k_{des}}{\overset{k_{ads}}{\rightleftharpoons}} N_2{-}* \qquad (1)$$

$$N_2{-}* + * \underset{k_{rec}}{\overset{k_{dis}}{\rightleftharpoons}} 2N{-}* \tag{2}$$

and are illustrated by the potential diagrams in fig. 1 for activated adsorption (fig. 1a) and for non-activated adsorption (fig. 1b). The kinetic parameters underlying the model with non-activated adsorption were derived from single crystal data for Fe(111) at low coverages [4–7,22] and are listed in table 1. According to these data $E_{dis} < E_{des}$, so that the effective activation energy for dissociative chemisorption, E^*, is even slightly negative as shown in fig. 1b [6,7].

The difference between the two approaches is that Stoltze and Nørskov [18–20] assumed the dissociation of $N_{2,ads}$ to form N_{ads} to be rate-determining. The equilibrium constants for the other elementary steps were derived using statistical mechanics. Dumesic and Trevino [21], on the other hand, made no assumptions on

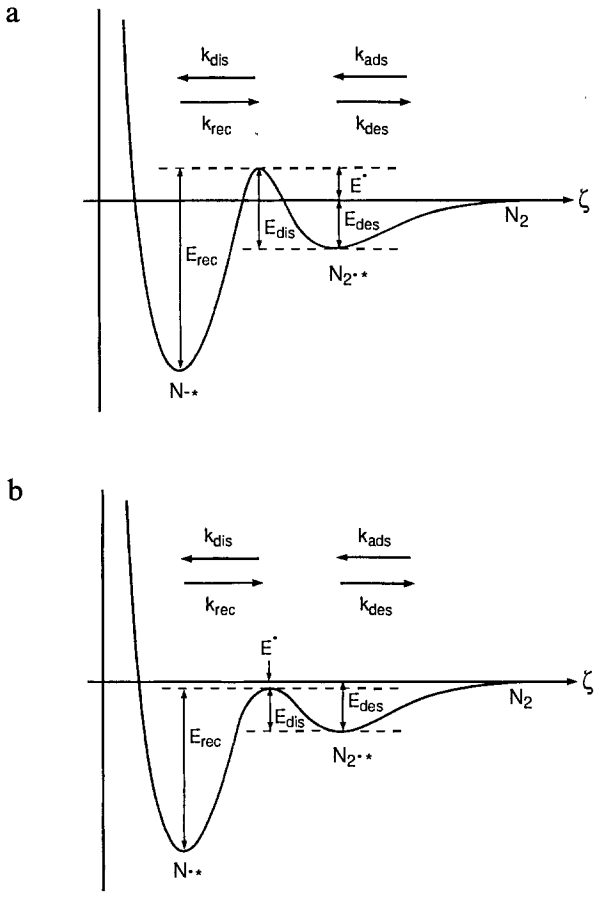

Fig. 1. (a) Schematic potential diagram illustrating activated adsorption/desorption of N_2 on the iron based NH_3 catalyst. (b) Schematic potential diagram illustrating non-activated adsorption/desorption of N_2 on the iron based NH_3 catalyst.

Table 1
Preexponential factors and activation energies of the Stoltze–Nørskov model for the rate constants $k_i = A_i \exp(-E_i/RT)$ [21]

$A_{rec} = 1.32 \times 10^9\ s^{-1}$	$E_{rec} = 155.0\,kJ/mol$	$A_{dis} = 4.29 \times 10^9\ s^{-1}$	$E_{dis} = 28.5\,kJ/mol$
$A_{des} = 1.87 \times 10^{14}\ s^{-1}$	$E_{des} = 43.1\,kJ/mol$	$A_{ads} = 3.33 \times 10^3\ Torr^{-1}\ s^{-1}$	$E_{ads} = 0.0\,kJ/mol$

the nature of the rate-determining step and used Arrhenius expressions for the rate constants of all elementary steps. The same approach was applied by Bowker et al. [8–11] who found good agreement between predicted and experimental rates following the kinetics of Scholten et al. [23] with a net activation barrier for dissociative N_2 chemisorption of $E^* = 50$ kJ/mol. All models assume only one type of active site and use Langmuir isotherms implying coverage-independent rate constants.

The total number of sites necessary for the present microkinetic analysis is determined experimentally by a new method developed recently [24]. According to this method, the number of sites results from the integration of the NH_3 peak generated by the temperature-programmed surface reaction (TPSR) between preadsorbed N_{ads} and H_2. The TPSR method has the advantage of measuring the area of the catalyst in the active state without any necessity to transfer the catalyst sample from the reactor to a static volumetric system like in the case of conventional CO chemisorption. The selective chemisorption of CO is usually used to determine the number of Fe surface atoms assuming a CO/Fe stoichiometry of 1/2 [2]. The amount of NH_3 formed in various TPSR experiments indicated that dosing N_2 at atmospheric pressure results in a stoichiometry of $N_{ads}/Fe = 1/1$ if normalized with the data from CO chemisorption [24]. Under UHV conditions the absolute value for the saturation coverage on Fe(100) was derived to be of $N_{ads}/Fe = 1/2$ [4,22]. The present study employs a similar experimental set-up as in ref. [24] with a mass spectrometer as universal detector calibrated quantitatively for the on-line analysis of N_2, H_2, NH_3, and H_2O. Both the highly sensitive detection system and highly purified gases are basic requirements for measuring N_2 TPD traces successfully.

2. Experimental

The experiments were carried out in an all stainless steel microreactor system with four gas lines which could be operated at pressures up to 100 bar. The gases used had the following purities: He 99.9999%, N_2 99.9999%, H_2 99.9999%, the mixture of 25% N_2 in H_2 used as synthesis feed gas 99.9996%. The feed gas was further purified by means of a self-designed guard reactor [25]. The flows were controlled by electronic mass flow meters and the temperatures by microprocessor controllers. The reactor consisted of a glass lined U-tube similar to the one described in ref. [26]. No desorption of N_2 or H_2 could be detected from the empty tube within the limits of detection. The U-tube was placed in a copper block which could be heated

up to 900 K. Gas analysis was performed by a mass spectrometer (Balzers GAM 445) which was calibrated for He, H_2, N_2 and NH_3 by using a reference gas mixture. The calibration for H_2O was carried out using a He stream saturated with H_2O at room temperature.

The catalyst used was a multiply promoted iron-based KM1 catalyst supplied by Haldor Topsøe A/S. The BET area determined on-line after reduction was 12.9 m^2/g. Usually 300 mg of the 250–800 μm sieve fraction were used resulting in a bed height of 15 mm which prevented limitations by heat or mass transport [27]. The reduction was carried out in synthesis gas using 40 Nml/min with a heating ramp of 10 K/h up to 720 K. After 48 h at 720 K the concentration of H_2O was below the detection limit of 1 ppm and the concentration of NH_3 had reached a stable value. The absence of poisoning by oxygen-containing compounds was tested as described in ref. [25]. NH_3 synthesis could be run at steady state at temperatures as low as 540 K.

When analysing the N_2 TPD experiments the design equation of a continuous flow stirred tank reactor (CSTR) was used:

$$\frac{p_{N_2}}{p_0} = -\frac{S}{F}\frac{d\theta_{N_{ads}}}{2dt} = -\frac{S\beta}{F}\frac{d\theta_{N_{ads}}}{2dT}, \tag{3}$$

where p_{N_2} is the partial pressure of N_2, p_0 is the ambient pressure, S is the total number of sites, $\theta_{N_{ads}}$ is the coverage of N_{ads} ranging from 0 to 1, F is the carrier flow rate in number of molecules/s, β is the heating rate in K/s. This equation is a good approximation for sufficiently small heating rates and a high amount of inert carrier gas [28]. The heating rate was 5 K/min, if not stated otherwise, and the He flow was 50 Nml/min resulting in a maximum concentration of about 200 ppm N_2.

3. Results and discussion

Prior to carrying out a N_2 desorption experiment NH_3 synthesis was run at steady state. Then the gas composition was changed from the stoichiometric synthesis gas mixture to only N_2 at the same temperature. After dosing N_2 for 60 min the temperature was lowered to room temperature within 40 min. At room temperature the flow was switched to He and the catalyst was flushed for another 40 min before the temperature ramp was started.

Initially, at 600 K a steady state NH_3 synthesis rate of 0.28 μmol/s g was recorded which decreased to 0.24 μmol/s g after completion of the first TPD experiment up to 870 K. After the third and all following TPD experiments the rate was found to be 0.22 μmol/s g. The catalyst was cooled immediately after reaching 870 K in order to minimize the time spent at that high temperature.

Typical TPD data recorded after dosing N_2 at different temperatures are reproduced in fig. 2. When dosing at 670 K trace A was obtained which displays a peak

at about 650 K. In addition to the desorption of N_2 a broad H_2 peak was observed at about 780 K which presumably originated from the decomposition of residual NH_x species. Since its area was only about 10% of that of the N_2 peak, its influence on the N_2 peak shape was considered to be negligible. The N_2 signal continues to rise to higher temperature indicating the segregation of atomic nitrogen from the bulk to the surface followed by recombination and desorption. This was further investigated by lowering the temperature again after the end temperature of 870 K had been reached. The experiment was repeated without additional dosing of N_2 (trace B). The partial pressure of N_2 starts to rise from 800 K and reaches 60 ppm at 870 K.

When dosing N_2 at 600 K (trace C) the N_2 concentration was found to increase less strongly at high temperature. In addition to the peak at 644 K which is now more pronounced, a broad shoulder appears at about 770 K. Repeating the TPD experiment without further exposure to N_2 results in a less strongly rising signal reaching only 30 ppm at 870 K. This observation is in agreement with the temperature dependence of the solubility of atomic nitrogen in Fe which is known to

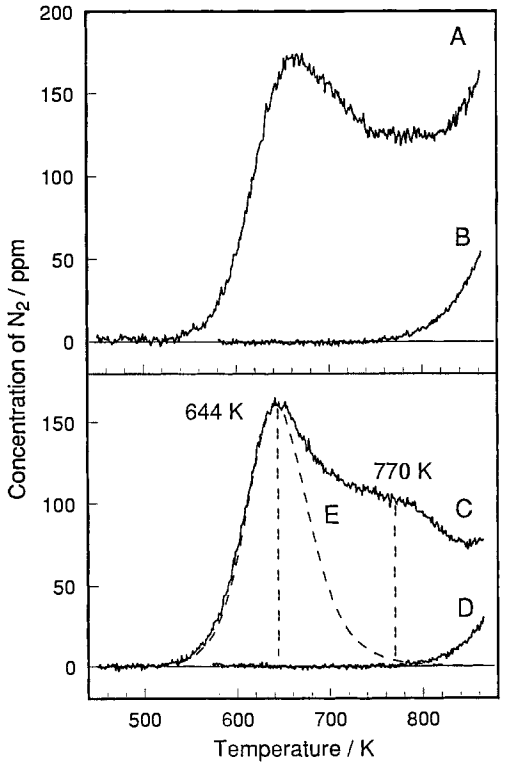

Fig. 2. N_2 TPD spectra obtained by dosing N_2 at 670 K (trace A) and at 600 K (trace C) followed by cooling in N_2. Traces B and D result from repeating the TPD experiment without additional dosing of N_2 after experiments A and C, respectively. Trace E was calculated based on second-order desorption without readsorption using $k_{rec} = 1 \times 10^9\ s^{-1} \exp\{-(146\ kJ/mol)/RT\}$.

increase with increasing temperature [29,30]. The amount of N segregating from the bulk seems to exceed the maximum equilibrium solubility of 0.3 μmol/g [29]. However, dissolved atomic nitrogen is presumably also located in higher concentrations at grain boundaries which are known to act as fast diffusion paths for the exchange between adsorbed and dissolved atomic nitrogen.

Due to the interference with segregation of dissolved nitrogen at high temperature it is difficult to assess whether saturation was achieved at the lower dosing temperature. This question could be clarified by applying the TPSR method yielding roughly the same amount of 94 μmol N_{ads}/g at both temperatures. Based on the ratio $Fe/N_{ads} = 1/1$ the amount of 94 μmol Fe/g corresponds to a specific surface area of 8.0 m^2/g assuming the Fe(111) atom density of 0.7×10^{19} Fe atoms/m^2.

By applying Bodenstein's stationary principle for the surface intermediate $N_{2,ads}$, i.e., by setting $dN_{2,ads}/dt = 0$, and by neglecting adsorption from the gas phase, the rate of desorption assuming Langmuir kinetics according to eqs. (1) and (2) is given as

$$-\frac{d\theta_{N_{ads}}}{2dt} = \frac{k_{des}k_{rec}\theta^2_{N_{ads}}}{k_{des} + k_{dis}(1 - \theta_{N_{ads}})} . \tag{4}$$

Due to the largely different preexponentials, $A_{des} >> A_{dis}$, (cf. table 1 and refs. [6,7]), also $k_{des} >> k_{dis}$, even if $E_{dis} < E_{des}$, and eq. (4) simplifies to

$$-\frac{d\theta_{N_{ads}}}{2dt} = k_{rec}\theta^2_{N_{ads}} , \tag{5}$$

i.e. the recombination of chemisorbed nitrogen atoms is rate-limiting for desorption. Analysis of the leading edge of the TPD trace of fig. 2C in terms of this approach by starting with the kinetic parameters as listed in table 1 yielded the best fit for an only slightly modified set of parameters, namely $A_{rec} = 1 \times 10^9$ s^{-1} and $E_{rec} = 146$ kJ/mol, as displayed by trace E in fig. 2. This is considered as strong evidence for assigning the TPD peak at 644 K to N_2 desorption resulting from recombination of chemisorbed nitrogen atoms.

Subtracting the calculated second-order TPD peak at 644 K (fig. 2E) from the experimental TPD spectrum (fig. 2C) results in a broad peak centered at about 770 K. Comparing its full width at half maximum (FWHM) of 170 K with the FWHM of 80 K of the calculated TPD peak shows that it cannot be modelled by second-order desorption without readsorption unless a broad distribution of desorption states is assumed. The origin of the shoulder at 770 K has to be attributed to the fact that during the thermal desorption experiment the partial pressure of N_2 is not negligible so that particularly with a porous solid readsorption has to be taken into account. By inclusion of the step

$$N_2 + * \rightarrow N_2{-}* \tag{6}$$

into the analysis, trace A in fig. 3 results which displays a shoulder at about 635 K

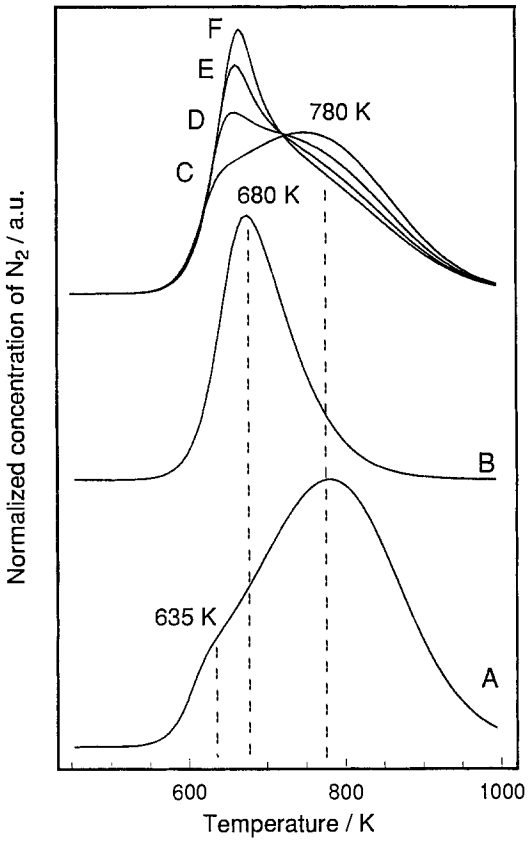

Fig. 3. Results of N_2 TPD simulations for the present flow system based on the Stoltze–Nørskov rate constants. Trace A was calculated including readsorption. Trace B was obtained by using a net activation energy for dissociative chemisorption of +15 kJ/mol. Traces C–F result from using a coverage-dependent net activation energy for dissociative chemisorption increasing from −15 kJ/mol by 10, 20, 30, and 40 kJ/mol, respectively.

due to desorption under kinetic control, i.e., without readsorption, and a broad maximum at 780 K due to desorption under thermodynamic control, i.e., with readsorption occurring. Increasing the activation energy of dissociation E_{dis} to 58 kJ/mol which is equivalent to a positive net activation energy of adsorption $E^* = 1$ kJ/mol leads to trace B. Now the broad peak at 780 K disappeared and only an asymmetric peak shape to higher temperature indicates the influence of readsorption. The shape of traces A and B suggests that the experimental peak shape can be satisfactorily modelled by modifying the set of rate constants tabulated in table 1. Since both a peak at 644 K and a broad shoulder at about 770 K are observed experimentally, a coverage-dependent net activation energy for dissociative chemisorption was introduced which is assumed to increase linearly with coverage while the preexponentials were kept constant as the most practical approximation. With the full set of steps as illustrated by fig. 1 and by assuming

establishment of the equilibrium $N_2 + * \rightleftharpoons N_2{-}*$ which is justified since $k_{des} >> k_{dis}$ the rate of desorption is given by

$$-\frac{d\theta_{N_{ads}}}{2dt} = k_{rec}\theta^2_{N_{ads}} - k_{dis}\theta_{N_{2,ads}}\theta_* \tag{7}$$

with

$$K_{des} = \frac{p_{N_2}\theta_*}{\theta_{N_{2,ads}}} \tag{8}$$

and

$$\theta_* = \frac{1 - \theta_{N_{ads}}}{1 + p_{N_2}/K_{des}} \tag{9}$$

leading to

$$-\frac{d\theta_{N_{ads}}}{2dt} = k_{rec}\theta^2_{N_{ads}} - \frac{k_{dis}k_{ads}}{k_{des}} p_{N_2} \frac{(1 - \theta_{N_{ads}})^2}{(2 + p_{N_2}/K_{des})^2} . \tag{10}$$

Since $p_{N_2}/K_{des} << 1$, this simplifies to

$$-\frac{d\theta_{N_{ads}}}{2dt} = A_{rec} \exp(-E_{rec}/RT)\theta^2_{N_{ads}} - \frac{A_{dis}A_{ads}}{A_{des}} \exp\{-[E_{dis} + (E_{ads} - E_{des})]/RT\} p_{N_2}(1 - \theta_{N_{ads}})^2 . \tag{11}$$

Hence it is the net preexponential factor $A^* = A_{dis}A_{ads}/A_{des}$ and the net activation energy for dissociative chemisorption $E^* = E_{dis} + (E_{ads} - E_{des})$ which determine the influence of readsorption on the peak shape. It is reasonable to assume that both the activation energy and the preexponential factor vary with coverage. However, the available data set does not allow a unique separation of the contributions from both parameters. In order to work with a model as simple as possible only E^* was assumed to be coverage dependent. In the following, only E^* is assumed to vary with coverage. Traces C–F in fig. 3 were obtained by using linearly increasing net activation energies of adsorption:

$$E^* = -15 \text{ kJ/mol} + E_{inc}\theta . \tag{12}$$

The values chosen for E_{inc} were 10, 20, 30, and 40 kJ/mol, respectively. An increasing value for E_{inc} increases the height of the peak without readsorption and reduces the height of the shoulder at high temperature. The experimental peak shape resembles closely traces D and E. Experimentally, the assumption underlying the analysis can be tested by varying the heating rate and the initial coverage as shown in figs. 4 and 5, respectively. The measured raw data are shown as dotted traces whereas the solid lines result from the simulation. Comparing traces A–C in fig. 4 which were obtained by using heating rates of 1, 5, and 10 K/min reveals that T_{max} shifts with increasing heating rate to higher temperature (table 2). The

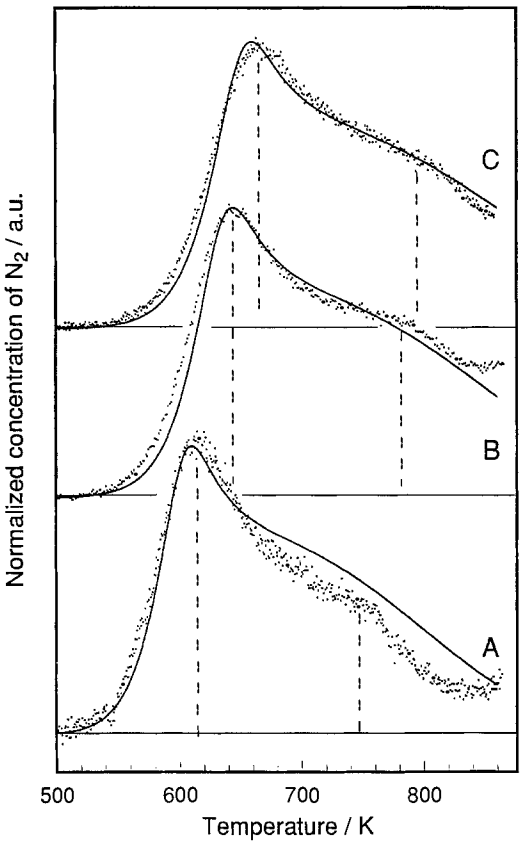

Fig. 4. Heating-rate variation: the normalized experimental data are shown as dots, the solid lines are the results of the simulation using equation (13). Traces A, B, and C were obtained by using $\beta = 1, 5,$ and 10 K/min, respectively.

height of the peaks at T_{max} scales linearly with the heating rate as shown in table 2. The amount of N_2 desorbed was obtained by integrating up to the end temperature of 870 K. The integration is complicated by the segregation of dissolved nitrogen from the bulk as manifested by fig. 2. On the other hand, the simulation of the N_2 desorption indicates that the desorption extends to temperatures even higher than 870 K. Since the average amount of N_2 desorbed of 41 μmol/g agrees roughly with the amount of 94 μmol NH_3/g formed during the TPSR experiment, the integration seems to work reasonably, i.e., both effects seem to cancel when integrating to 870 K.

Plotting $\ln(T_{max}^2/\beta)$ versus $1/T_{max}$ yields $k = 2 \times 10^9$ s^{-1} exp{ − (146 kJ/mol)/RT} by applying linear regression, in excellent agreement with the value $k = 1 \times 10^9$ s^{-1} exp{ − (146 kJ/mol)/RT} obtained from modelling the leading edge of the 5 K/min peak (trace E in fig. 2). The position of the broad peak shifts to higher temperature and its height relative to the peak maximum at lower temperature

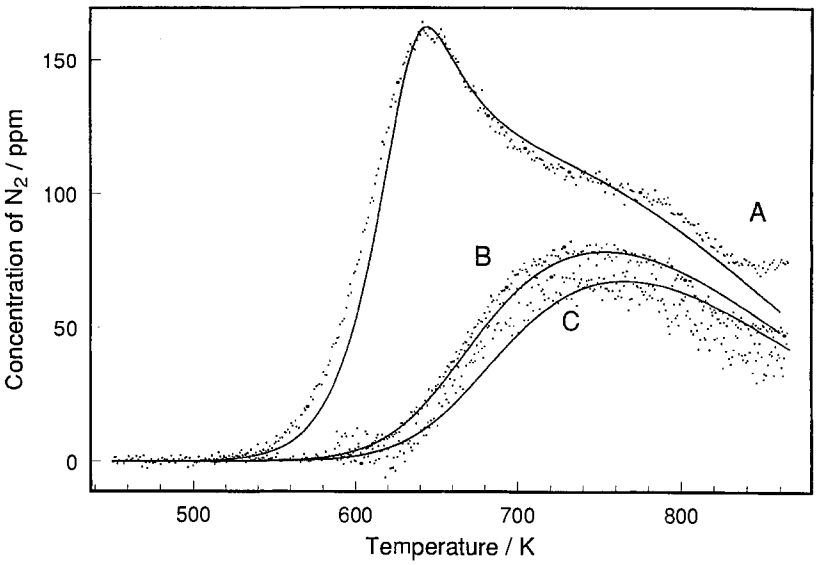

Fig. 5. Variation of initial coverage using a heating rate of 5 K/min: trace A was obtained by dosing N_2 at 600 K and subsequent cooling in N_2 to achieve full coverage. Trace B was obtained after cooling in synthesis gas to 300 K. Trace C results from changing from synthesis gas to He at 540 K.

increases with increasing heating rate. These observations are in line with the assignment of the broad peak to desorption with readsorption occurring since the increasing heating rate leads to a higher transient partial pressure of N_2 in the gas phase which in turn increases the rate of readsorption.

When starting the TPD experiment with $\theta_{N_{ads}}$ far below saturation, then free sites are available which prevent the desorption of N_2 without readsorption. Correspondingly, only the broad peak at higher temperature is observed as shown in

Table 2
Experimental results of varying the heating rate and the initial coverage. Traces A, B and C in fig. 4 were obtained by using $\beta = 1, 5, 10$ K/min, respectively, dosing at 600 K. In fig. 5, a heating rate of 5 K/min was chosen. Trace A results from N_2 dosing at 600 K and subsequent cooling in N_2 to achieve saturation. Trace B results from cooling in synthesis gas to 300 K, trace C results from changing from synthesis gas to He at 540 K

Trace		Heating rate (K/min)	T_{max} (K)	N_2 concentration at T_{max} (ppm)	Amount of N_2 (μmol/g)
fig.4	A	1	615	33	41
	B	5	644	160	44
	C	10	666	285	38
fig.5	A	5	644	160	44
	B	5	750	78	21
	C	5	750	66	17

fig. 5 (traces B and C). In addition to the experimental parameters its position depends on the initial coverage. Trace A was obtained by dosing N_2 at 600 K and cooling subsequently in N_2 to achieve saturation. Trace B results from a cooling experiment in synthesis gas to room temperature during which H_2 and N_2 compete for the empty sites. The achieved coverage of N_{ads} is difficult to predict since in addition to the relative rates of adsorption also the rate of removal of N_{ads} as NH_3 has to be taken into consideration. During the subsequent TPD experiment also the desorption of H_2 was observed from room temperature on as expected from the codosing procedure. The desorption of H_2 below the onset of N_2 desorption creates empty sites which in turn increase the rate of N_2 readsorption. The amount of N_2 desorbed of 21 μmol/g yields $\theta = 0.5$ in good agreement with $\theta = 0.6$ determined by the modelling.

Trace C was obtained after running NH_3 synthesis at 543 K. At this temperature the steady state coverage of N_{ads} is assumed to be far less than saturation. Then the flow was switched to He and the catalyst was flushed for 170 min to remove H_{ads} before the TPD experiment was started. The amount of N_2 desorbed should thus be correlated to the steady state coverage of N_{ads} under synthesis conditions due to the relatively small rate of desorption at the flushing temperature of 543 K. Dividing the amount of 17 μmol N_2/g desorbed in experiment D by the amount in experiment B yields a coverage of 0.4 in satisfactory agreement with a coverage of 0.55 determined by the modelling.

All traces in figs. 4 and 5 were simulated using the following rate equation:

$$-\frac{d\theta_{N_{ads}}}{2dt} = 3 \times 10^8\ s^{-1} \exp\{-(143.5\ kJ/mol)/RT\}\theta_{N_{ads}}^2 - 7.64 \times 10^{-2}\ Torr^{-1}\ s^{-1} \exp\{-[(-14.6 + 29.7\theta)kJ/mol]/RT\} \times p_{N_2}(1 - \theta_{N_{ads}})^2 . \quad (13)$$

Taking the simplified reactor design equation into account, the agreement between experiment and simulation is considered to be rather good. The key conclusion is that all five TPD experiments were simulated successfully using the same value of 30 kJ/mol for E_{inc}. The coverage-dependent activation energy for adsorption implies that the heat of dissociative N_2 adsorption is coverage-dependent, too. Its value is given by $(E_{dis} - E_{des}) - E_{rec}$, i.e., it is decreasing from its initial value of −161 kJ/mol to −131 kJ/mol at full coverage. The value used for k_{rec} differs slightly from the value obtained by varying the heating rate due to the influence of the coverage-dependent net activation energy of adsorption. This indicates that the actual dependence on the coverage could be more complicated than the assumed linear relationship. Scholten et al. [31,23] observed a steep rise at low coverage and an essentially constant value at higher coverage. Such a type of coverage-dependence would reduce the influence of readsorption on the rising part of the

TPD trace where the coverage is still high. However, the linear dependence seems to be the most reasonable assumption as long as single crystal measurements on promoted Fe(111) at high coverage are not available.

Formally, the linear dependence of E^* on coverage is equivalent to a linear distribution of sites with varying E^*. The linear dependence is also used in the derivation of the Frumkin–Temkin isotherm. For Fe(100) and Fe(111) the activation energy of the sticking coefficient is known to increase with increasing coverage of N_{ads} [4]. Hence the obtained increase of 30 kJ/mol is qualitatively in agreement with single crystal studies but it is far below the value of 96 kJ/mol at high coverage observed by Scholten et al. [31,23]. Furthermore, the rate constant $k_{rec} = 10^{13}\ s^{-1} \exp\{-(134\ kJ/mol)/RT\}$ used by Bowker [11] would result in a slightly asymmetric N_2 TPD peak at 450 K under our conditions including readsorption in the simulation. This is clearly not the case.

The rate constant of recombination $k_{rec} = 1.32 \times 10^9\ s^{-1} \exp\{-(155\ kJ/mol)/RT\}$ used in the Stoltze–Nørskov model reproduces the results obtained in UHV reasonably well as shown by Dumesic and Trevino [21]. In the present study $k_{rec} = 2 \times 10^9\ s^{-1} \exp\{-(146\ kJ/mol)/RT\}$ was derived. However, when using this value for k_{rec} to calculate the outcome of a TPD experiment with $\beta = 10$ K/s at saturation under UHV conditions a N_2 TPD peak at 753 K results compared with about 850 K observed by Bozso et al. [4] on Fe(111). The higher rate of desorption for the industrial catalyst may actually be due to the presence of the promoter potassium which is thermally stabilized by coadsorbed oxygen [32]. It is a consequence of the principle of microscopic reversibility that the enhanced rate of dissociation of $N_{2,ads}$ due to potassium results *also* in an enhancement of the rate of recombination which, as shown in the derivation of equation (5), determines the rate of N_2 desorption. Further studies are in progress to clarify this conjecture [33].

On Fe(111), Fe(110) and Fe(100) the N_2 desorption maxima were observed at about 850, 910 and 930 K, respectively, using a heating rate of 10 K/s [5]. One should therefore expect that under the present conditions the presence of all three faces on the catalyst surface should give rise to at least two discernible N_2 TPD peaks. The good agreement between the observed TPD traces and the simulation using only one N_{ads} species suggests that mainly Fe(111) planes are exposed to the gas phase which are promoted uniformly by the K + O adlayer.

Based on the present peak assignment earlier results in the literature indicate that in these studies full coverage was not achieved and thus only the peak at high temperature with readsorption occurring was observed. Amenomiya et al. [34] employing the KM1 catalyst found the peak maximum temperature to be located between 770 and 820 K depending on the amount adsorbed. The heating rate used was 16 K/min. Vandervell et al. [14] cooled a triply promoted iron catalyst in synthesis gas to 78 K. Correspondingly, a peak maximum temperature of 800–820 K was observed similar to trace B in fig. 4 using a heating rate of 15 K/min.

The impact of the present results on the microkinetic model for steady-state

NH_3 synthesis is threefold. First, the rate of N_2 desorption was found to be somewhat higher than assumed in the Stoltze–Nørskov model based on UHV experiments. Secondly, the coverage-dependent net activation energy of adsorption reduces the rate of N_2 adsorption at high coverage. These two effects will qualitatively decrease the rate of NH_3 synthesis. Thirdly, since the activation energy for recombination of two N_{ads}, E_{rec}, is kept constant while E^* for adsorption increases with coverage, there will be a net lowering of the adsorption energy for nitrogen, providing a higher concentration of free sites which causes an increase of the rate of NH_3 synthesis.

4. Conclusions

N_2 TPD experiments were carried out in a microreactor system operating at atmospheric pressure. The observed peak structure consisting of a narrow peak at 644 K followed by a broad shoulder at about 770 K was identified as arising from desorption mainly without readsorption at low temperature and mainly with readsorption at high temperature. Varying the heating rate resulted in a shifting peak maximum temperature yielding a preexponential factor $A_{rec} = 2 \times 10^9$ molecules/site s and an activation energy $E_{rec} = 146$ kJ/mol in excellent agreement with values for k_{rec} determined by modelling the rising part of the TPD peak assuming second-order desorption without readsorption. The observed rate constant is in satisfactory agreement with $A_{rec} = 1.32 \times 10^9$ molecules/site s and $E_{rec} = 155$ kJ/mol derived by Dumesic and Trevino [21] on the basis of the Stoltze–Nørskov model [18–20].

Higher heating rates increased the partial pressure of N_2 and also the amount of N_2 desorbing at higher temperature. Starting the TPD experiments with coverages far below saturation gave rise to the peak at higher temperature only. Both observations support the assignment of the peak at higher temperature to desorption of N_2 with readsorption occurring since the rate of readsorption is proportional to p_{N_2} at θ_*.

Simulating N_2 TPD curves using the model by Stoltze and Nørskov revealed that the calculated TPD curves were not influenced by the molecular precursor to desorption. However, the calculated rate of readsorption was found to be overestimated at high coverage compared with the experimental results. Simulation of the experimental data was successfully achieved by using a linearly increasing net activation energy for dissociative chemisorption of N_2 as simplest assumption:

$$E^* = (-15 + 30\theta_{N_{ads}})\ \text{kJ/mol}. \tag{14}$$

It would be interesting to use the modified parameters derived in the present study for the full microkinetic analysis of NH_3 synthesis.

Acknowledgement

The authors benefited from discussions with B. Fastrup, E. Törnqvist and R. Schlögl and are grateful to Haldor Topsøe A/S for supplying the iron catalyst. The software to simulate the TPD experiments was kindly developed by M. Wesemann.

References

[1] J.R. Jennings, ed., *Catalytic Ammonia Synthesis*, 1st Ed. (Plenum Press, New York, 1991).
[2] M. Boudart and G. Djéga-Mariadassou, *Kinetics of Heterogeneous Catalytic Reactions*, 1st Ed. (Princeton Univ. Press, Princeton, 1984).
[3] R. Schlögl, R.C. Schoonmaker, M. Muhler and G. Ertl, Catal. Lett. 1 (1988) 237.
[4] F. Bozso, G. Ertl, M. Grunze and M. Weiss, J. Catal. 49 (1977) 18.
[5] F. Bozso, G. Ertl and M. Weiss, J. Catal. 50 (1977) 519.
[6] G. Ertl, S. Lee and M. Weiss, Surf. Sci. 114 (1982) 515.
[7] G. Ertl, S. Lee and M. Weiss, Surf. Sci. 114 (1982) 527.
[8] M. Bowker, I. Parker and K.C. Waugh, Appl. Catal. 14 (1985) 101.
[9] M. Bowker, I. Parker and K.C. Waugh, Surf. Sci. 197 (1988) L223.
[10] I. Parker, K.C. Waugh and M. Bowker, J. Catal. 114 (1988) 457.
[11] M. Bowker, Catal. Today 12 (1992) 153.
[12] C.T. Rettner and H. Stein, Phys. Rev. Lett. 59 (1987) 2768.
[13] C.T. Rettner and H. Stein, J. Chem. Phys. 87 (1987) 770.
[14] H.D. Vandervell and K.C. Waugh, Chem. Phys. Lett. 171 (1990) 462.
[15] M. Muhler, L.P. Nielsen and B. Fastrup, Chem. Phys. Lett. 181 (1991) 380.
[16] K.C. Waugh, D. Butler and B.E. Hayden, Catal. Lett. 24 (1994) 197.
[17] M. Muhler, L.P. Nielsen, E. Törnqvist, B.S. Clausen and H. Topsøe, Catal. Lett. 14 (1992) 241.
[18] P. Stoltze and J.K. Nørskov, Phys. Rev. Lett. 55 (1985) 2502.
[19] P. Stoltze and J.K. Nørskov, Surf. Sci. 197 (1988) L230.
[20] P. Stoltze, Phys. Scripta 36 (1987) 824.
[21] J.A. Dumesic and A.A. Trevino, J. Catal. 116 (1989) 119.
[22] R. Imbihl, R.J. Behm, G. Ertl and W. Moritz, Surf. Sci. 123 (1982) 129.
[23] J. Scholten, P. Zwietering, J. Konvalinka and J. de Boer, Trans. Faraday Soc. 55 (1959) 2166.
[24] B. Fastrup, M. Muhler, H.N. Nielsen and L.P. Nielsen, J. Catal. 142 (1993) 135.
[25] B. Fastrup and H.N. Nielsen, Catal. Lett. 14 (1992) 233.
[26] T.Z. Srnak, J.A. Dumesic, B.S. Clausen, E. Törnqvist and N.-Y. Topsøe, J. Catal. 135 (1992) 246.
[27] A. Nielsen, J. Kjaer and B. Hansen, J. Catal. 3 (1964) 68.
[28] J.A. Dumesic, D.F. Rudd, L.M. Aparicio, J.E. Rekoske and A.A. Trevino, *The Microkinetics of Heterogeneous Catalysis*, ACS professional reference book (Am. Chem. Soc., Washington, 1993).
[29] H.J. Grabke, Z. Phys. Chem. NF 100 (1976) 185.
[30] W. Mahdi, J. Schütze, G. Weinberg, R.C. Schoonmaker, R. Schlögl and G. Ertl, Catal. Lett. 11 (1991) 19.
[31] J. Scholten and P. Zwietering, Trans. Faraday Soc. 53 (1957) 1363.
[32] Z. Paal, G. Ertl and S.B. Lee, Appl. Surf. Sci. 8 (1981) 231.
[33] M. Muhler, F. Rosowski, B. Fastrup and G. Ertl, to be published.
[34] Y. Amenomiya and G. Plezier, J. Catal. 28 (1973) 442.